Journal Pre-proof

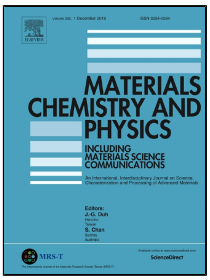

Electromagnetic shielding properties of epoxy composites with hybrid filler nanocarbon/$BaTiO_3$

Ludmila Vovchenko, Oleg Lozitsky, Ludmila Matzui, Viktor Oliynyk, Volodymyr Zagorodnii, Mykola Skoryk

PII:	S0254-0584(19)31049-1
DOI:	https://doi.org/10.1016/j.matchemphys.2019.122234
Reference:	MAC 122234
To appear in:	*Materials Chemistry and Physics*
Received Date:	31 March 2018
Accepted Date:	28 September 2019

Please cite this article as: Ludmila Vovchenko, Oleg Lozitsky, Ludmila Matzui, Viktor Oliynyk, Volodymyr Zagorodnii, Mykola Skoryk, Electromagnetic shielding properties of epoxy composites with hybrid filler nanocarbon/$BaTiO_3$, *Materials Chemistry and Physics* (2019), https://doi.org/10.1016/j.matchemphys.2019.122234

Electromagnetic shielding properties of epoxy composites with hybrid filler nanocarbon/$BaTiO_3$

Ludmila Vovchenko*[1], Oleg Lozitsky[1], Ludmila Matzui[1], Viktor Oliynyk[2], Volodymyr Zagorodnii[2], Mykola Skoryk[3]

Department of Physics[1] and Department of Radiophysics, Electronics, and Computer Systems[2], Taras Shevchenko National University of Kyiv, Volodymyrska str., 64/13, Kyiv, 01601, Ukraine
G. V. Kurdyumov Institute for Metal Physics of the NAS of Ukraine[3], Vernadskiy Str. 36, Kyiv, Ukraine

**Correspondence : vovch@univ.kiev.ua*

Abstract

The investigation of the electromagnetic shielding properties of composites based on epoxy resin L285 and hybrid filler graphite nanoplatelets/$BaTiO_3$ particles (GNP/BT) has been performed in the frequency range of 1–67 GHz. The experimental study involved measuring direct current (DC*)* conductivity, complex permittivity (versus frequency), and shielding properties of such composite materials with 0, 3, 5 and 6 wt.% contents of graphite nanoplatelets and 35 wt.% of $BaTiO_3$ particles in the composite. The significant increase of permittivity was observed in the ternary epoxy composites GNP/BT/epoxy with the increase of GNP content. The observed sufficient increase of electromagnetic radiation (EMR) shielding in K_a-band for high GNP content correlates with DC electrical conductivity increase. The simulation of the reflection loss in such composites in EMR frequency range of 1–67 GHz has been performed in C++ environment using experimentally determined permittivity frequency dependence. The influence of sample thickness on position, width, and depth of EMR absorption maximums was defined for the composites with 0, 3, 5 and 6 wt.% content of graphite nanoplatelets and 35 wt.% of $BaTiO_3$ filler. [1]

[1] **List of abbreviations**

CM — composite material; GNP — graphite nanoplatelet; BT — $BaTiO_3$; DC - direct current L285 — epoxy resin Larit285; H285 — hardening agent H285; AR — aspect ratio; EMR — electromagnetic radiation; SE_T — EMR shielding efficiency; SE_R — shielding due to reflection; SE_A — shielding due to absorption; RL — reflection loss.

Keywords: graphite nanoplatelets; nanocomposite; electrical conductivity; permittivity; electromagnetic shielding.

1. Introduction

The development of new polymer composites filled with various nanoparticles presents one of the important tasks of modern applied science. Nanofillers have a great effect on polymer properties as the nano-size of such particles implies a high surface area that leads to a high interfacial area with the polymer and to the formation of filler networks at very low nanofiller content. The new enhanced properties of polymer composites filled with carbon nanoparticles (carbon nanotubes, graphite nanoplatelets, graphene) make these composites suitable for mechanical deformation sensor (piezoresistive) [1], electromagnetic interference material [2-4], anti-electrostatic coating too. In recent years the research on microwave absorption materials has attracted intensive attention to improving the attenuation of electromagnetic radiation. It has been shown in [5, 6] that nanometer-scaled multi-walled carbon nanotubes (MWCNTs) are a remarkably high-performance functional microwave absorption material due to the combined light weight and remarkable mechanical and electronic properties [7]. However, very often, the homogeneous distribution of the nanosized particles is problematic due to strong Van der Waals interactions among the nanofiller themselves [8]. On the other hand, the good conductivity of carbon nanoparticles used as a microwave absorbing material has the shortcoming of poor impedance matching. In order to overcome these main problems, magnetic and dielectric materials may be favorable to improving the impedance matching of carbon nanoparticles [9]. Last time an increasing interest is for polymer-based composites with hybrid filler systems, for example, a carbon nano-filler combined with carbon black (CB) [10], metal or metal oxide particles [11-13], various dielectric nanoparticles such as TiO_2 [14, 15], MoS_2, $BaTiO_3$ nanoparticles [16-19]. Such a combination of nanocarbon filler and inorganic nanoparticles promotes the further improving the absorption performance of nanocarbon–filled polymers and also enhances the mechanical properties and thermal stability. It was shown in [20] that three-dimensional (3D) conductive network structures formed by

barium titanate/carbon nanotubes incorporated polyaniline were favorable for electromagnetic absorption capability enhancement. In addition, these composites with hybrid fillers may be used for the fabrication of the high-efficient microwave absorbing materials by designing of the multi-layer structures. Such multi-layered absorbers allow to decrease the EM reflection at the first boundary air/shield and increase the absorption of EMR inside the shield due to multi-reflections on layers interfaces. The absorption enhancement, which was produced by the multi-layered structure, may be tuned by variation of the filler content in each layer [21].

There are many papers devoted to the investigation of dielectric properties of polymer composites filled with hybrid filler nanocarbon/dielectric particles in the frequency range of 1 Hz-1 MHz. So, the use of high aspect ratio fillers is a promising route to provide high dielectric constant, low loss materials at a low filler volume fraction, for use as capacitors and electric field grading materials. It was shown in [22] that a combination of ferroelectric barium titanate and graphene platelets used in a polydimethyl siloxane matrix yielded high dielectric constant in 1 Hz – 1 MHz range of frequencies. Poly (vinylidene fluoride) (PVDF) matrix hybrid nanocomposites, featuring barium titanate (BT) nanoparticles and multi-walled carbon nanotubes (MWCNT) embedded in the polymer, showed the good distribution of the ceramic nanoparticles with very little particle agglomeration [23]. The conductive MWCNT increased the charge storage ability of the polymer matrix by serving as a polarized charge transport phase for the ferroelectric nanoparticles, while the used small MWCNT amount prevented the formation of conductive networks. The dielectric properties of the polymer matrix nanocomposites with hybrid fillers (BT with and without MWCNT) were improved by optimizing the synergistic effects between the charge storage behavior of the ferroelectric phase and the charge transport behavior of the conductive phase. Concerning microwave properties of polymer composites with combined nanocarbon/dielectric filler particles, there are few publications and EMR frequency range is limited by 18 GHz [9, 18, 20, 24]. That is why the purpose of this work is to investigate the effect of the combination of $BaTiO_3$ nanoparticles and GNPs filling the epoxy matrix on the complex permittivity

of such ternary composites in the wide microwave range (1 – 67 GHz) and to study the shielding properties of developed composites.

2. Experimental

2.1 Materials

Graphite nanoplatelets (GNPs) and dielectric ultra-disperse particles of $BaTiO_3$ (BT) were used as fillers for the preparation of nanocomposites. $BaTiO_3$ powder was purchased from Materials Lab Inc, Ukraine. GNPs were obtained by thermo-exfoliation of oxidized natural graphite with the following ultrasonication in acetone medium for 3 hrs [25, 26]. GNPs are disk-shaped plates with the lateral dimensions of 10 μm and the average thickness of 40 nm. Low-viscosity epoxy resin Larit285 (viscosity of 600÷900 mPa×s, the density of ~1.20 g/cm^3 (at 25°C)) with hardening agent H285 (viscosity of 50÷100 mPa×s) was used as a polymer matrix.

2.2 Preparation of composites

GNPs/epoxy and GNP/BT/epoxy CMs with 3-6 wt.% of GNPs and 35wt.% of BT were fabricated by the method of mixing in solution with additional sonication. At first, an appropriate amount of epoxy resin was pre-dissolved with acetone. Further, GNPs or GNP/BT were introduced into the epoxy solution and carefully mixed. After this, the dispersing in BAKU ultrasonic bath with the frequency of 40 kHz and power of 50 W was applied for 2 hrs. Finally, curing agent H285 was added in an amount of 40 % by weight of the L285 and the composite mixture was subjected to mechanical mixing. For preparing the samples with the desired form the composite mixture was poured into Teflon forms and samples were cured at room temperature during 1 day. After that, for the complete polymerization, the samples were treated at the temperature that gradually increased from 40 to 80^{0}C for 5 hrs.

Structural and morphological peculiarities of the filler particles and epoxy composites with such fillers have been studied by optical microscopy (“Mikmed-1” with ETREK PCM-510 attachment), electron microscopy (JEOL JSM-6490LV; Mira3 Tescan), X-ray diffraction (DRON-4-07 X-ray diffractometer, filtered CoK_α-irradiation) at room temperature.

2.3 Measurements

The electric resistance of the investigated composites was measured by standard two- or four-probe method in DC mode at room temperature with a limit of measurement of electric resistance of 10^{10} ohm. Higher than 10^{10} ohm, resistances were measured using teraommetr E6–13. Samples for measurements were prepared in the form of regular parallelepipeds with the dimensions 7.0 × 3.0 × 3.0 mm^3.

Conductivity (σ) was calculated accounting the dimensions of samples by:

$$\sigma = \frac{1}{R}\frac{l}{S}, \quad (1)$$

where R is the measured resistance, l is the length of the sample or the distance between electrodes, and S is the cross-sectional area of the sample.

The complex permittivity (ε_r', ε_r'') spectra were measured by Keysight PNA N5227A vector network analyzer using the transmission–reflection method in the frequency range of 1–67 GHz. The permittivity was derived from the scattering parameters using the iterative procedure "NIST precision method" [27] by Agilent 85071E Material Measurement Software. For the measurements of scattering parameters the samples in the form of toroids with outer diameter of 1.85mm and a hole with a diameter of 0.82mm were machined using an ultra precise lathe. The samples tightly fit into the precise 1.85 mm coaxial airline. Full two-port calibration was initially performed on the test setup in order to remove errors due to the directivity, source match, load match, isolation, and frequency response in both the forward and reverse measurements.

The scalar network analyzer was used to measure the transmission index T and standing wave ratio (SWR) for GNP/BT/epoxy composites within the 25.5–37.5 GHz. Index T was determined as a ratio of detected signals corresponding to the electric field strengths of the incident E_I and transmitted E_T waves, $T = |E_T / E_I|^2$. Reflection index R can be determined from SWR [28]:

$$R = \left(\frac{SWR - 1}{SWR + 1}\right)^2 . \quad (2)$$

3. Results and Discussion

3.1 Sample Characterization

In order to define the quality of purchased $BaTiO_3$ powder as a filler (chemical composition, the morphology of the particles) XRD analysis and SEM electron microscopy were used. Figure 1 presents powder XRD patterns for $BaTiO_3$ powder.

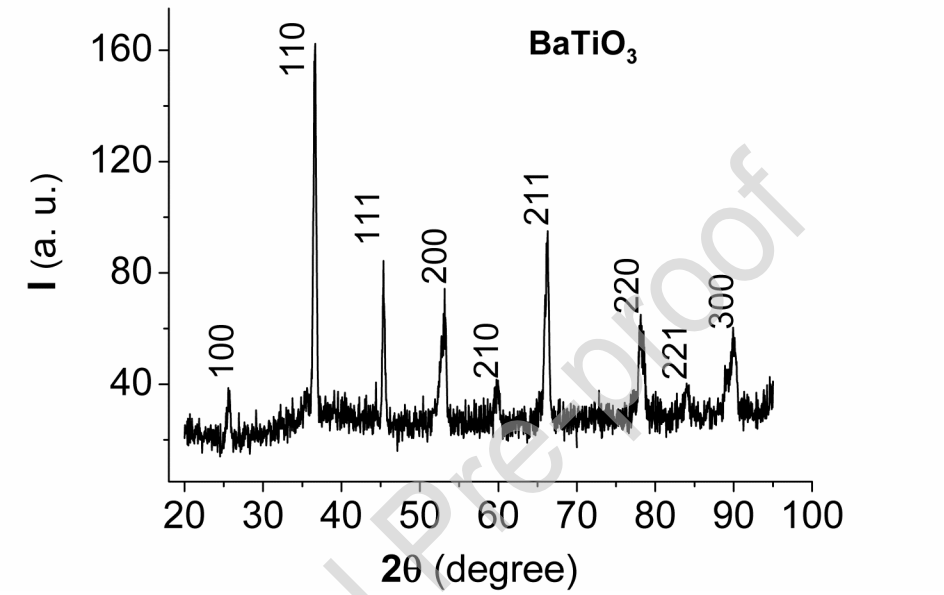

Figure 1. Diffractogram for the initial $BaTiO_3$ powder.

XRD result shows the powder of $BaTiO_3$ to be well-defined cubic crystal structure with smaller grain size, that confirmed by the symmetric (200) peak and absence of 002 peak (for the case of tetragonal perovskite structure) [22].

Figure 2 shows the SEM images of filler particles BT and GNPs.

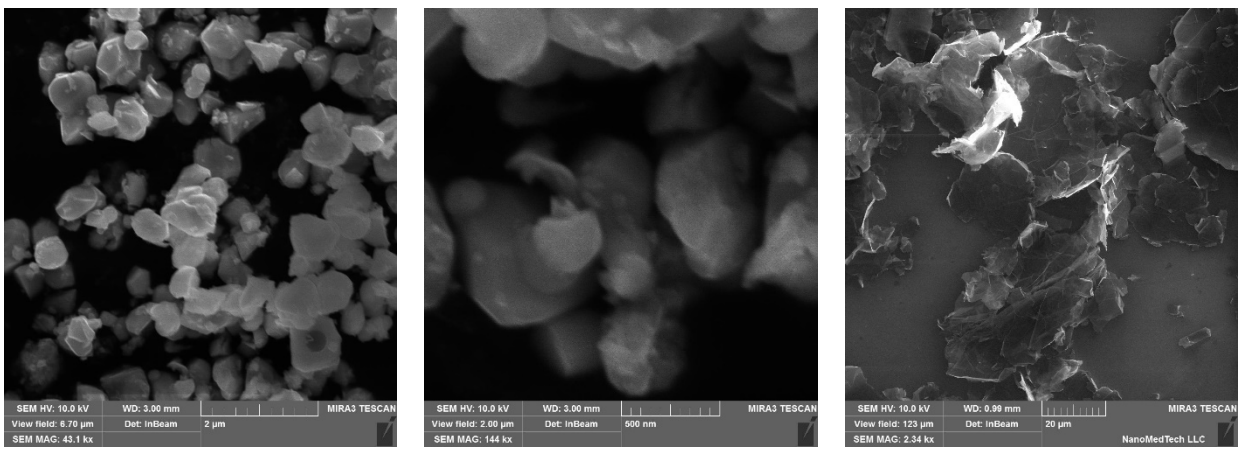

(a) (b) (c)

Figure 2. SEM-images of the disperse BT particles (a, b) and graphite nanoplatelets GNPs (c).

As it is seen from Fig. 2 a, b the size of BT particles varies in the range 150-700 nm, but the most number of BT particles have the size of 400 nm. The most part of GNP particles are of 10 μm in diameter, however, the large particles of 20–100 μm in diameter are observed as well (Fig. 2c). The actual thickness of the graphite nanoplatelets is over the range of 40 to 100 nm.

To determine the effect of a combination of two types of filler on dielectric and shielding properties of materials, a series of CM samples with a hybrid filler of GNP / BT for different weight concentrations of GNP and constant content of BT in CM were manufactured. The samples are respectively marked as xGNP/BT/L285, where x – weight content of GNP in CM, data is shown in Table 1.

Table 1. The phase composition and porosity of GNP/BT/epoxy CMs

	$BaTiO_3$, wt.%	GNP, wt.%	d, g/cm^3	Porosity, P	σ_{DC}, S/m
0GNP/BT/L285	34.5	0	1.40	0.12	$2.0 \cdot 10^{-11}$
3GNP/BT/L285	34.5	3	1.37	0.15	$1.36 \cdot 10^{-8}$
5GNP/BT/L285	34.5	5	1.41	0.14	$4.45 \cdot 10^{-5}$
6GNP/BT/L285	34.5	6	1.32	0.20	$1.30 \cdot 10^{-2}$

Figure 3 displays the surface SEM and cross-section SEM of GNP/BT/epoxy nanocomposites with various content of GNP particles. It can be observed in Fig. 3a for CM BT/epoxy that BT particles are mainly well-dispersed in the epoxy matrix. However, in some regions of the sample, we have observed the higher concentration of BT particles (see Fig. 3d). For CMs filled with GNP particles with the content of 3 and 5wt.% the BT particles in GNP/BT/epoxy nanocomposites are uniformly distributed on the GNPs surface (see Figs. 3b, c) and between GNP particles (see Figs. 3e, f).

As it is seen from the cross-section SEM images of GNP/BT/epoxy nanocomposites

(Figs. 3 e, f), the concentration of BT particles is higher compared with surface SEM images and some voids and pores can be clearly observed in these ternary composites. The uniform distribution of both types of filler particles in the investigated composites was also confirmed by the optical images presented in Figs. 3 g, h, i.

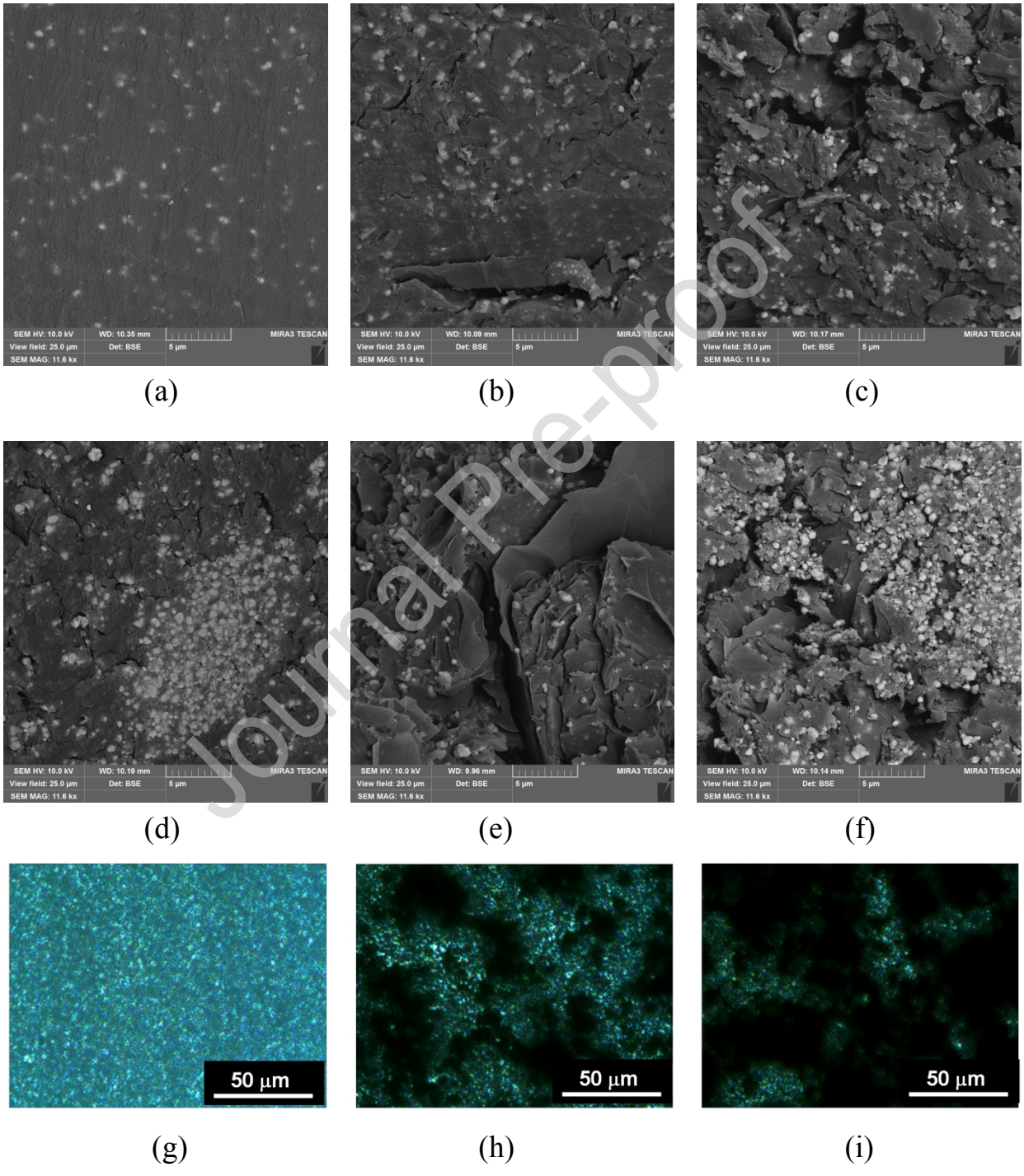

Figure 3. Surface SEM images (a-c), cross-section SEM images (d-f) and optical images (g-i) of the GNP/BT/epoxy nanocomposites: (a, d, g) - BT/epoxy, (b, e, h) - 3GNP/BT/epoxy, (c, f, i) - 5GNP/BT/epoxy.

The porosity of epoxy composites was determined using the following ratios:

$$P = 1 - \frac{d_{CM}}{d_{CM(id)}}, \qquad d_{CM(id)} = \left(\sum_{i=1}^{n} C_i / d_i \right)^{-1}, \tag{3}$$

where d_{CM} and $d_{CM(id)}$ – CM sample density and density of perfect sample without pores, accordingly, C_i, d_i are the weight fraction and density of the *i* component in composite, consisting of *n* components.

In determining the porosity of samples using proportions (1), the values of density of GNP, BT and epoxy were used as follows: (d_{GNP} =2.20 g/cm^3; d_{L285} =1.15 g/cm^3, d_{BT} =5.85 g/cm^3 [29].

It was found that the porosity of composites monotonically increased with GNP content, only the sample 5GNP/BT/epoxy has the porosity 0.14 that is lower compared with 3GNP/BT/epoxy sample. Such discrepancy may be explained by some manufacturing step mis-matching and rough method in determination of samples density via its volume and weight.

Table 1 also shows data on DC electrical conductivity of CMs, which, as can be seen from the table, increases significantly with increasing GNP content in the composite. As it is seen from the table 1 the electrical conductivity of more compact 5GNP/BT/epoxy sample is on 3 orders lower than for the 6GNP/BT/epoxy composite with higher porosity. This fact confirms the crucial role of conductive particle content in polymer composite for the formation of the conductive network, while in highly porous materials such as building materials based on concrete, carbon foams the porosity is an important parameter for the electrical conductivity, shielding and absorbing properties [30, 31]. For the investigated samples of composites GNP/BT/epoxy the size of pores and heterogeneity is smaller (see Fig. 3) compared with the wavelength of EMR in the frequency range 1-67 GHz, so these samples can be considered as uniform and isotropic materials.

3.2 Permittivity of GNP/BT/epoxy composites

Electromagnetic shielding and microwave absorption are two common strategies to resist the interference of incident electromagnetic waves, while they are generally evaluated by different measurement models.

For a conventional EMR shielding model, the most important thing is to attenuate the intensity of the transmission EM waves, and a common parameter — shielding efficiency (SE_T) — is employed to describe the relationship between the transmission wave and the incident wave. The physical significance of reflection loss in EMR shielding is the difference between the initial incident waves and those waves penetrating into the shielding materials.

For the model of microwave absorption, however, a metal substrate is placed to reflect the transmission waves. As a result, the transmission waves are always negligible in microwave absorption. Reflection loss (RL) herein means the difference between the initial incident waves and the final reflected waves. The final reflected waves include all back-propagation EM waves reflected at various surfaces and interfaces, and ideal microwave absorbing materials should weaken the reflected waves as much as possible.

On the basis of relative complex permittivity $\varepsilon_r^* = \varepsilon_r' - i\varepsilon_r''$ and relative complex permeability $\mu_r^* = \mu_r' - i\mu_r''$, the reflective and absorptive properties of a material can be deduced from the transmission line theory [32].

In a case of polymer composites filled with both non-magnetic conductive and ferroelectric particles, the microwave properties are determined by the complex permittivity ε_r^* and electrical conductivity σ_{DC} at high content of electroconductive filler.

Figure 4 shows the real ε_r' and imaginary ε_r'' parts of complex permittivity and dielectric loss tangent ($\tan\delta = \varepsilon_r'' / \varepsilon_r'$) for GNP/BT/epoxy composites in the frequency range of 1-67 GHz. For the comparison, the data for CMs filled with solely BT or GNP (3 and 5wt.% content) particles are also presented.

It was known [18] that the real part of complex permittivity ε_r' is the storage capacity of the surface charge when the composite is under an applied electric field.

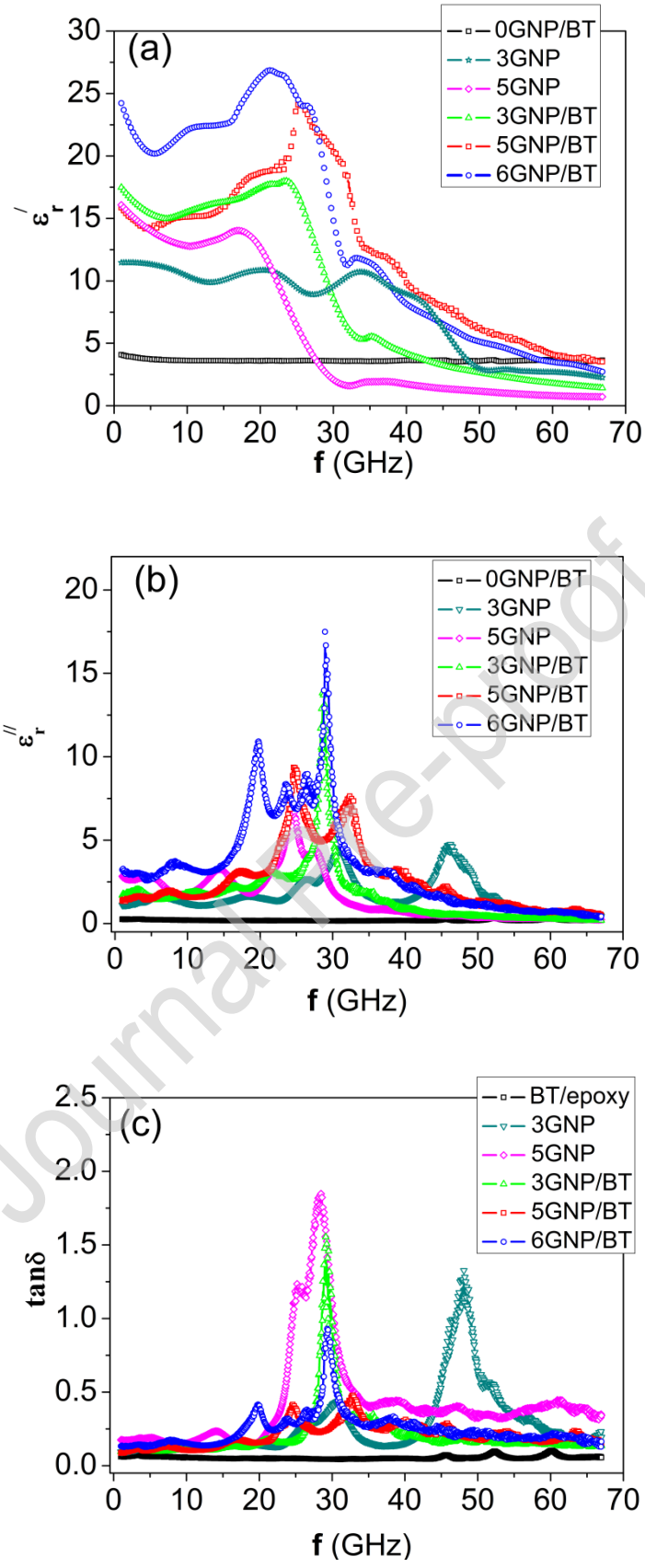

Figure 4. Complex permittivity and dielectric loss tangent of epoxy composites with single GNP filler and hybrid filler GNP/BT: a) real part of permittivity, b) imaginary part of permittivity, c) dielectric loss tangent.

The imaginary part of complex permittivity ε_r'' presents the energy loss in a dielectric medium. It can be seen in Fig. 4 that both the real and the imaginary parts of complex permittivity of BT/epoxy is relatively small (ε_r'~3.6, ε_r''~0.18) and remain constant within the range of 1-67 GHz resulting in negligible dielectric loss tangent ($\tan\delta$ ~0.06).

Such low permittivity value of BT/epoxy composite is explained by the low content of BT particles (only 35wt.% that corresponds to ~ 9 vol.%) and relatively low permittivity of BT particles with cubic structure compared to large ferroelectric BT particles with tetragonal structure [29].

Introduction of graphite nanoplatelets in polymer matrix results in a significant increase in dielectric constant and change in frequency dependence. For the sample with 3 wt.% GNP/L285 in 1–32 GHz frequency range ε_r' is 12-11.5. Starting at 33 GHz, ε_r' decreases with frequency up to 2.8. An increase in the GNP content to 5 wt% results in an increase of ε_r' to 15 and a similar dependence on the frequency of the EMR. The imaginary permittivity of these samples increases especially and reaches maximums at frequencies corresponding to ε_r' drops, and integrally decreases with a subsequent increase of frequency. These composites exhibit electrical heterogeneity as it comprises highly conductive graphite nanoparticles randomly dispersed in a low lossy dielectric epoxy matrix. Sufficiently high ε_r' for the epoxy CMs filled with graphite nanoplatelets at relatively low filler content is explained by the high aspect ratio (AR) of GNPs particles (AR ~ 200) and the large contribution of interfacial polarization [33, 34]. Under the action of an alternating electric field of EMR, the electric current must flow across the interface between the epoxy matrix and the GNPs. It results in the accumulation of charges at the interface. Accordingly, this leads to the formation of large dipoles at the GNP–epoxy interface, and the polarizability of the composite becomes stronger. As it was shown in our previous papers [35, 36], ε_r' of epoxy composites filled with GNPs may vary within 4-50 in the frequency range of 26-54 GHz depending on the filler content.

Compared to the GNP-filled composites, ε_r' and ε_r'' values of the ternary GNP/BT/epoxy composites were enhanced. This increase in ε_r' for the ternary composites may be related to the better dispersion of GNPs particles in the epoxy matrix in the presence of BT particles, which prevent GNPs agglomeration at CMs fabrication. In addition, the introduction of BT particles with relatively high (compared to epoxy resin) permittivity sufficiently increases the volume of interfacial regions BT–epoxy and enhances the role of interfacial polarization in the formation of effective permittivity of CM. As one can see in Fig. 4, the maximal values of ε_r' as well as ε_r'' were observed for the 6 wt.%GNP/BT/L285 CM. It can be ascribed to the "geometrical effect" of formed 3D conductive network structures of GNPs particles and the strong interfacial polarization effects enhanced between conducting GNP particles and epoxy matrix, leading to the rise of ε_r'. The nonsmooth curves for ε_r' frequency dependencies and presence of few peaks of ε_r'' for ternary CMs with 5 and 6 wt.% of GNPs can be explained by high heterogeneity of CM and indicate the existence of several dielectric polarization mechanisms that contribute to overall permittivity [37]. As it is seen from Fig. 4c, the maximum of dielectric loss tangent exceeds 1 that evidences the strong dielectric relaxation process for this frequency range. Such a high value of $\tan\delta$ is completely acceptable in this case of permittivity dispersion and was observed also for another carbon/polymer composites [38].

Thus, the values and frequency dependencies of GNP/BT/epoxy composites' complex permittivity can be adjusted simply by changing the filler content. The ability to manipulate these characteristics as well as designing of multi-layered shields based on composites with hybrid fillers are important to obtain good shielding and absorptive properties in the microwave range.

3.3 Microwave absorbing properties of GNP/BT/epoxy ternary composites

As it was mentioned above, the relative complex permittivity ε_r^* of polymer composite filled with conductive particles is a very important parameter that can determine its microwave absorption properties. Starting from the knowledge of the

permittivity, the absorbing properties of polymer filled composites can be analysed considering one-layer of given thickness (l), backed by a metallic plate. Reflection loss (RL) for this case was calculated using the following expression [39]:

$$RL = 20\lg\left|\left(Z_{in} - Z_0\right)/\left(Z_{in} + Z_0\right)\right|, \quad (4)$$

where $Z_{in} = Z_0\sqrt{\mu_r^*/\varepsilon_r^*}\tanh(\gamma \cdot l)$ is the input wave impedance at the air/composite interface, $Z_0 = \sqrt{\mu_0/\varepsilon_0} = 377\Omega$ is the free-space wave impedance.

To examine the absorbing properties of developed ternary GNP/BT/epoxy composites in the wide microwave range of 1-67 GHz, we have calculated the reflection loss RL (dB) for a normal incident wave at the surface of infinite thin-plate composite screen backed by a perfect conductor (metal) using Eq. (4) for two different thicknesses. Figure 5 shows a typical relationship between reflection loss and frequency for the samples of ternary GNP/BT/epoxy CMs with different thicknesses (1 and 2.5 mm).

As it is seen, RL depends on the GNP content in CMs as that content variation produces changes in ε_r' and ε_r'' values and their frequency dependences. It is also seen from the figure, that the few $RL_{\min}$ are observed in the frequency range 1-67 GHz.

From equation (4) and expression for Z_{in}, a minimum reflection requires a perfect matching between permittivity, permeability, frequency, and thickness of the composite material with the free space. Since the μ_r^*=1 for GNP/BT/epoxy CMs, for the samples with the same thickness, the reflection loss minimums for the present GNP–epoxy composites are mainly determined by the matching condition of permittivity of the composites at a certain frequency f_m. This matching frequency f_m that corresponds to $RL_{\min}$ is related to matching thickness d_m by following expression [40]:

$$f_m = \frac{n}{4} \cdot \frac{C_0}{d_m \cdot \sqrt{|\mu_r \cdot \varepsilon_r|}}, \; n = 1,\ 3,\ 5\ . \quad (5)$$

Composites with relatively high GNP loadings have higher dielectric permittivities and RL minimums are shifted into lower frequency range.

Figure 5a shows at 31 GHz the wide reflection loss minimum RL_{min} - 7.8 GHz at −10 dB level for 3GNP/BT/epoxy CM plate of 1 mm thickness.

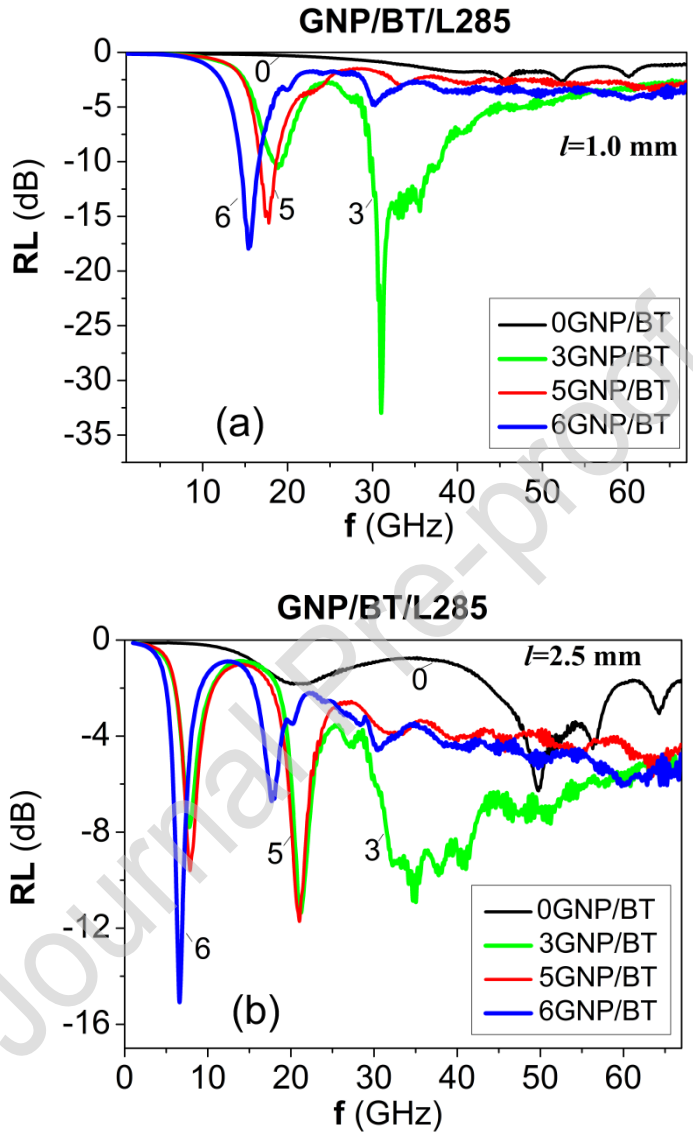

Figure 5. The calculated values of the reflection loss (RL) versus EMR frequency for the ternary GNP/BT/epoxy composites with various content of carbon filler for shield thickness of 1 mm (a) and 2.5 mm (b) (the numbers on curves mean the GNP content in wt.%).

Our calculations of RL for various thickness of composite plate allow to suggest that such width of this RL_{min} is the result of the superposition of two RL_{min} - one due to so-called “geometrical effect” [40] when the thickness of absorbers satisfies Eq. (5)

and another RL_{min} is related to the maximum of dielectric loss tangent $\tan\delta$ at ~ 31 GHz, that was observed for 3GNP/BT/epoxy CM (see Fig. 4c). The increase of sample thickness up to 2.5 mm leads to the shift of RL minimums towards lower frequencies, the occurrence of new peaks in RL, and depletion of RL minimums.

Table 2 shows the absorbing properties for polymer composites filled with nanocarbon filler or mixed nanocarbon/inorganic fillers (backed by a conducting layer) which are presented in the literature.

Table 2. The reflection loss for polymer composites filled with single nanocarbon filler or mixed nanocarbon-based filler.

Composition	Sample thickness, mm	Band frequency, GHz	*RL*, dB	Ref.
15wt.GNP/epoxy	3	8-20	-14.5 (at 18.9 GHz)	[34]
2.6vol.% r-GO/PEO	1.8	16.4	-40	[41]
15wt.%BT/epoxy	3	1-15	-6 (12.5 GHz)	[42]
	4		-12 (11 GHz)	
70wt.%(BT@Ni)-PVDF+PANI	2	2-18	-22.6 (at 12.7 GHz)	[43]
20wt.%CNT@BT-PANI /wax	3	1-15	-28.9 (at 10.7 GHz)	[44]
1wt.%MWNT + 2vol.%(BT-GO)/PVDF/ABS	5	8-18	-44.9 (at 15.9 GHz)	[45]
3wt.%GNP/30wt.%BT/epoxy	1	1-67	-37 (at 31 GHz)	This
	2.5		-18 (at 16 GHz)	work
6wt.%GNP/30wt.%BT/epoxy	1	1-67	-12(at 21 GHz)	This
	2.5		-12 (at 38 GHz)	work

GO – graphite oxide, r-GO – reduced graphite oxide, MWNT – multi-walled carbon nanotubes, PEO – polyethylene oxide, PVDF - polyvinylidene fluoride, PANI – polyaniline, ABS - acrylonitrile butadiene styrene, (PEK) - poly(ether ketone).

As it is seen from table 2, the mixing of electric (GNP, r-GO, CNT, Ni) nanoparticles with highly dielectric $BaTiO_3$ particles sufficiently extend the possibility of

enhancement of microwave absorbing properties of polymer-filled composites at relatively low shields' thickness (in 1-3 mm). As it is seen from table 2, the reported in the literature data are restricted by the band frequency lower than 18 GHz, while the novelty of our results for GNP/BT/epoxy composites consists in the extension of the research into the frequency range up to 67 GHz. And it was found that among all tested GNP/BT/epoxy composites the sample 3wt.%GNP/30wt.%BT/epoxy exhibits a good absorption ability in the range 30-40 GHz at sample's thickness of 1 mm, while the increase of the GNP content up to 6 wt.% promotes the decrease of $RL_{\min}$ value due to the higher value of the EMR reflection index related to the increased complex dielectric permittivity of such composites.

3.4 Shielding properties of GNP/BT/epoxy ternary composites

In order to estimate the shielding properties of ternary composites GNP/BT/epoxy, we have determined EMR reflection and transmission indices when electromagnetic waves penetrate through the shield material. There are three mechanisms that determine the effectiveness of EMR shielding. Part of the incident radiation energy is reflected from the front surface of the screen material, the other part is absorbed in the screen material, and the next part is reflected from the back surface of the screen. The latter part can either enhance the screening effectiveness or weaken depending on the phase shift of waves at the screen material interface. Thus, the total material shielding efficiency (SE_T) is equal to the sum of the shielding due to absorption (SE_A), reflection (SE_R), and multiple reflection (SE_I):

$$SE_T = SE_A + SE_R + SE_I \ . \quad (6)$$

The last mentioned factor is significant in thin high-conductivity screens or in low-loss screens when $SE_A \leq$ 10-15 dB [46].

All components of the equation are expressed in decibels. In practice, SE_I can be neglected in calculations of SE_T if $SE_A \geq 10$ dB.

Values SE_T, SE_R, and SE_A are expressed through indices of absorption A, reflection R, and transmission T, which are related with energy balance equation as

$A+T+R=1$ [47], as follows [48]:

$$SE_T=-10\lg T;\ \ SE_R=-10\lg(1-R)\ ;\ \ SE_A=-10\lg\left(\frac{T}{1-R}\right). \qquad (7)$$

Figures 6-7 show the frequency dependences of total EMR shielding efficiency and shielding due to the processes of EM waves reflection and absorption in the composites with binary GNP/BT filler. Samples thicknesses are ~ 1 mm and 2.5 mm.

As one can see from the shown data, the smallest attenuation of the EMR is observed for the sample of 35 wt.% BT/L285. The introduction of the GNP into the composite results in the growth of EMR attenuation. The attenuation increases with the GNP content in GNP/BT/L285 ternary CMs as well as with the sample thickness. Such increase of EMR shielding with the increase of GNP content correlates with the increase in the CM electrical conductivity and, correspondingly, with the increase in microwave electric losses. A conductive network of GNP particles is formed at high concentrations of carbon filler.

As it can be seen from Figs. 6c, 7c, the smallest EMR absorption SE_A occurs in samples of 35 wt.%BT/epoxy and the main contribution to EMR attenuation makes the reflection. In this case, increasing the sample thickness does not significantly affect the effectiveness of EMR shielding. A significant increase in EMR attenuation (SE_T) in the CM with an increase of GNP content occurs due to increased reflection (SE_R) as well as the significant increase in EMR absorption (SE_A).

As can be concluded from Fig. 8a, b, the contribution to EMR attenuation due to EMR absorption is higher than at the expense of EMR reflection and increases with the increase of the GNP content.

The efficiency of EMR reflection and absorption processes in a particular environment is defined by the parameters of the material itself (complex permittivity ε_r^* and permeability μ_r^*) as well as by that material thickness.

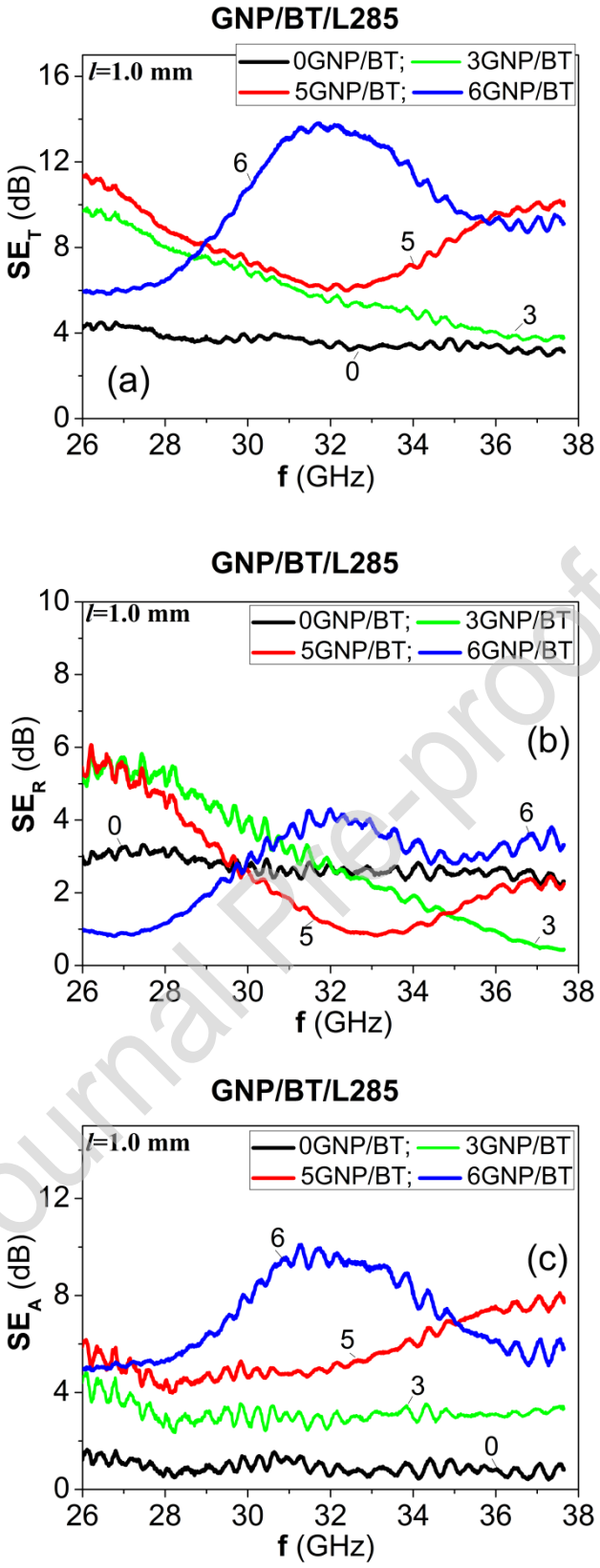

Figure 6. Total EMR shielding SE_T (a) and shielding due to reflection SE_R (b) and absorption SE_A (c) versus frequency for GNP/BT/epoxy CMs with various GNP content, the thickness of shield is 1 mm (the numbers on curves mean the GNP content in wt.%).

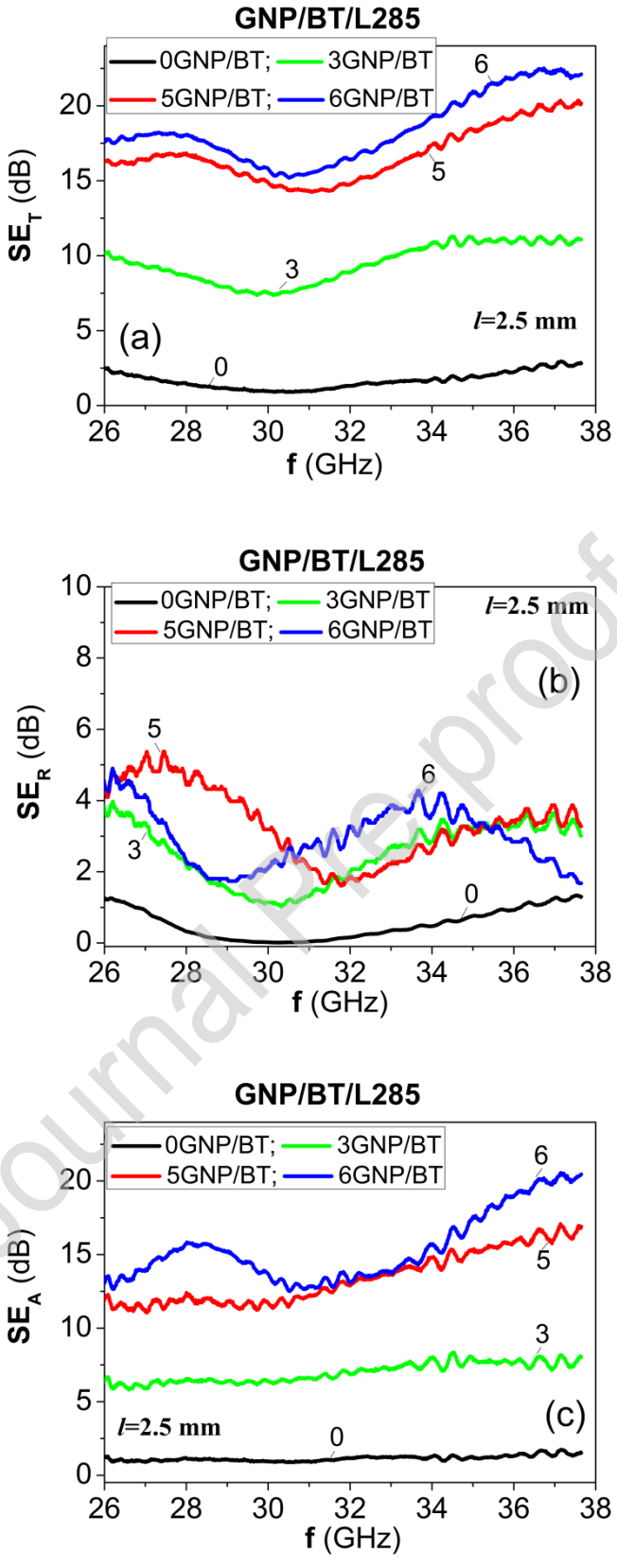

Figure 7. Total EMR shielding SE_T (a) and shielding due to reflection SE_R (b) and absorption SE_A (c) versus frequency for GNP/BT/epoxy CMs with various GNP content, the thickness of shield is 2.5 mm (the numbers on curves mean the GNP

content in wt.%).

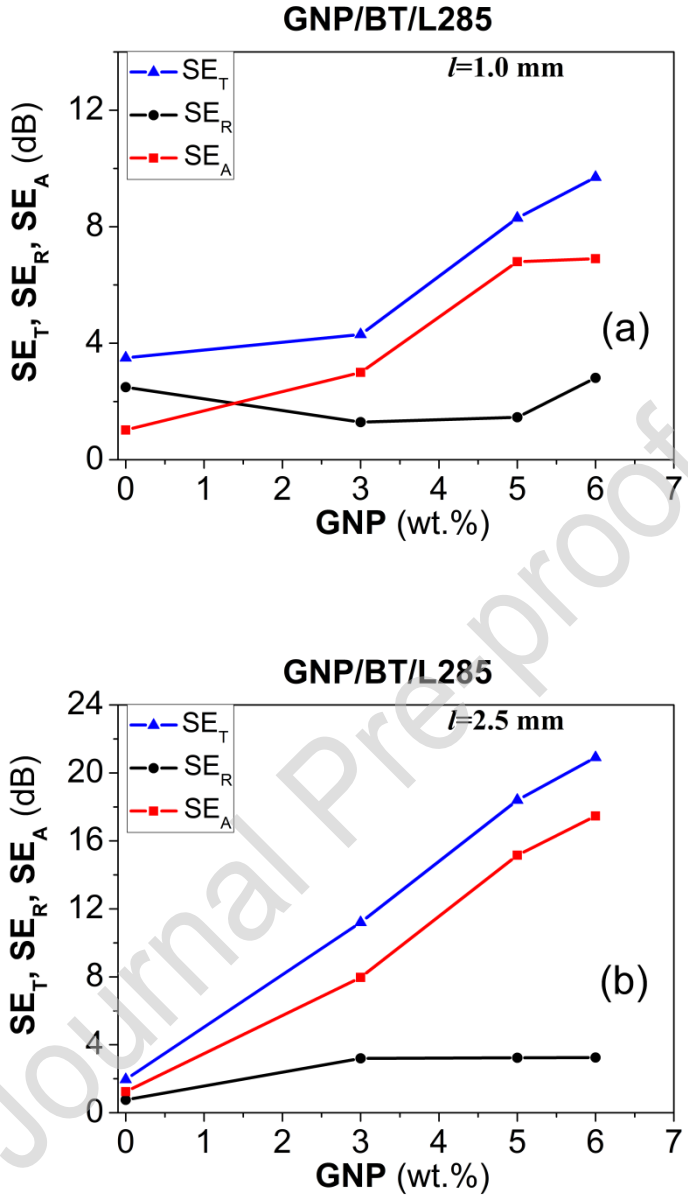

Figure 8. EMR shielding for GNP/BT/epoxy CMs versus GNP content at the frequency 35 GHz and various sample thickness, 1 mm (a) and 2.5 mm (b).

In the general case, the EMR shielding efficiency SE_T (in dB) is defined by the following expression [32, 49]:

$$SE_T = -10\lg|T| = 20\lg\left|e^{\gamma\cdot l}\right| + 20\lg\frac{\left|(1+n)^2\right|}{4|n|} + 20\lg\left|1-\frac{(1-n)^2}{(1+n)^2}\cdot e^{-2\gamma\cdot l}\right| \qquad (8)$$

$$= SE_A + SE_R + SE_I ,$$

where $n = k_z / k_0$ is the complex index of refraction; $k_0 = 2\pi/\lambda_0$ is the wavenumber in free space, $\lambda_0 = C_0/f$; λ_0 and f are the wavelength and the frequency; C_0 =3·10^8 m/s; $k_z = k_0 \cdot \sqrt{\varepsilon_r^* \mu_r^*}$; $\gamma = \alpha + i\beta$ is the complex propagation constant of electromagnetic wave (β is the phase constant, α is the absorption index); l is the shielding material thickness.

As it is illustrated in Figs. 6-8, an increase in the sample thickness from 1 to 2.5 mm leads to SE_T increase caused mainly by EMR absorption term because $SE_A \sim \lg e^{\gamma l} \sim \gamma l$ (see Eq. 8). In this case, the increase in SE_A can be attributed to the higher amount of free charge carriers in a thicker sample, that can interact with the penetrating EM radiation.

Table 3 lists out the EMI shielding properties of polymer composites filled with nanocarbon and nanocarbon/BT.

Table 3. EMI shielding properties of polymer composites filled with single nanocarbon filler or mixed nanocarbon-based filler.

Composition	Sample thickness, mm	Band frequency, GHz	SE_T, dB	Ref.
6wt.%GNP/ PBAT	1	8-12	5	[50]
15wt.%GNP/ PBAT			13	
15wt.%r-GO/PS	2	18	21.4	[51]
5vol.%GNP/PP/PE	1	8-12	5	[52]
3vol.%GNP/2vol.%CNT/PP/PE	1	8-12	13	[52]
10wt.%(GNP/CNT)/PU	3	12.4-18	47	[53]
7 wt% (GNP/CF)/epoxy	2	26.5-40	25	[54]
30wt.% BT/PEK	2	8.2-12.4	7.5	[55]
20vol.%$BaTiO_3$/10vol.%Ag/PVDF	1.2	8-12	26	[56]
1wt.%MWNT + 1vol.%(BT-GO)/PVDF/ABS	5	8-18	26	[45]
16wt.%(Graphene-Fe_3O_4-	2	1-20	35	[57]

$BaTiO_3$)/Silicone Rubber				
3wt.%GNP/30wt.%BT/epoxy	1	25.5-37.5	10-4	This
	2.5		10	work
6wt.%GNP/30wt.%BT/epoxy	1	25.5-37.5	6-14-9	This
	2.5		17.5-22	work

PBAT - poly(butylene adipate-*co*-terephthalate), PS – polystyrene, PP – polypropylene, PE – polyethylene, PU – polyurethane, PEK - poly(ether ketone).

As it is seen from table 3, the incorporation of single nanocarbon filler or mixed carbon (or nanocarbon) filler effectively increases the shielding properties of such composites. The combination of nanocarbon filler with dielectric or magnetic nanoparticles promotes the increasing of shielding due to increased SE_A absorption term at lower nanocarbon content compared with CMs with a single nanocarbon filler. Such enhancement of shielding properties of ternary compounds can be explained by better carbon nanoparticles dispersing in the polymer matrix (the lower level of nanocarbon particles agglomeration) in the presence of BT particles and by the increase of the volume of BT-polymer interfacial regions and effective internal multiple EMR reflection on interphase boundaries carbon-BT, BT-polymer and carbon-polymer.

4. Conclusion

Ternary epoxy composites filled with a mixture of GNPs and $BaTiO_3$ particles with different filler weight percent were prepared as microwave shielding materials. It was found that the increase of the GNPs content sufficiently enhances the microwave permittivity of ternary CMs. It was shown that permittivity of CMs with combined GNP/BT filler is higher compared to CMs with single GNPs filler. Such improvement of ternary compounds dielectric properties can be explained by better GNPs particles dispersion in the epoxy matrix in the presence of BT particles and by the increase of the volume of BT-epoxy interfacial regions. The latter enhances the role of interfacial polarization in the formation of effective material permittivity. Nonsmooth ε_r' frequency dependencies and occurrence of peaks in ε_r'' frequency

dependencies for ternary CMs with 5 and 6wt.% of GNPs can be explained by high heterogeneity of CMs and indicate the existence of several dielectric mechanisms that contribute to permittivity.

The reflection microwave loss RL (dB) of ternary GNP/BT/epoxy CMs was calculated. 3GNP/BT/epoxy CMs of 1 mm thickness exhibited reflection loss peak value of -30 dB at 31 GHz with wide absorption bandwidth (Δf =7.8 GHz).

The study of EMR shielding properties of ternary composites in Ka-band has shown that the introduction of highly conductive GNP particles in epoxy resin significantly increases the shielding efficiency due to effective processes of the reflection and absorption of microwaves. Such increase of EMR shielding efficiency at GNP content increase in CMs correlates with the enhancement of electrical conductivity and dielectric loss when the conductive network of GNP particles is formed at the high content of GNP filler.

The ability to manipulate the complex permittivity value and its frequency dependence varying the filler content in GNP/BT/epoxy composites seems important to achieve perfect microwave shielding properties.

Declarations

Funding

This research did not receive any specific grant from funding agencies in the public, commercial, or not-for-profit sectors.

Competing Interests

The authors declare that they have no competing interests.

Authors' Contributions

OL and LV fabricated the epoxy composites samples, carried out the optical microscopy investigation and measurements of the electrical resistivity. MS performed the investigation of the microstructure of composite samples using electron microscopy. OL and VZ carried out microwave measurements and wrote the manuscript. OL and LV carried out the calculations. LV and LM proposed the initial work, supervised the analysis, and revised the manuscript. All authors read and approved the final manuscript.

Acknowledgements

Not applicable.

Author details

Department of Physics & Department of Radiophysics, Electronics, and Computer Systems, Taras Shevchenko National University of Kyiv, 64/13 Volodymyrska Str., Kyiv 01601, Ukraine.

G. V. Kurdyumov Institute for Metal Physics of the NAS of Ukraine, Vernadskiy Str. 36, Kyiv, Ukraine

References

1. L. Shen, F. Wang, H. Yang, Q. Meng, The combined effects of carbon black and carbon fiber on the electrical properties of composites based on polyethylene or polyethylene/polypropylene blend, Polym Test 30 (2011) 442-448. https://doi.org/10.1016/j.polymertesting.2011.03.007

2. F. Qin, C. Brosseau, A review and analysis of microwave absorption in polymer composites filled with carbonaceous particles, J Appl Phys. 111 (2012) 061301. https://doi.org/10.1063/1.3688435

3. Yong Li, Song Zhang, Yuwei Ni, Graphene sheets stacked polyacrylate latex composites for ultraefficient electromagnetic shielding, Mater Res Express 3 (2016) 075012. https://doi.org/10.1088/2053-1591/3/7/075012

4. L. Vovchenko, Yu. Perets, I. Ovsienko, L. Matzui, V. Oliynyk, V. Launetz, Shielding coatings based on carbon-polymer composites, Surface and Coatings Technology 211 (2012) 196-199. https://doi.org/10.1016/j.surfcoat.2011.08.018

5. A.P. Sobha, P.S. Sreekala, S.K. Narayanankutty, Electrical, thermal, mechanical and electromagnetic interference shielding properties of PANI/FMWCNT/TPU composites, Progress in Organic Coatings 113 (2017) 168-174. https://doi.org/10.1016/j.porgcoat.2017.09.001

6. A.W. Orbaek, A.C. Owens, C.C. Crouse, C.L. Pint, A.R. Barron, Single walled carbon nanotube growth and chirality dependence on catalyst composition, Nanoscale 5 (2013) 9848-59. DOI: 10.1039/c3nr03142j

7. Y. Qing, Y. Mu, Y. Zhou, F. Luo, D. Zhu, W. Zhou, Multiwalled carbon nanotubes-$BaTiO_3$/silica composites with high complex permittivity and improved electromagnetic interference shielding at elevated temperature, Journal of the European Ceramic Society. 34 (2014) 2229-2237. https://doi.org/10.1016/j.jeurceramsoc.2014.02.007

8. N. Saba, P. Tahir, M. Jawaid, Review on Potentiality of Nano Filler/Natural Fiber Filled Polymer Hybrid Composites, Polymers 6 (2014) 2247-2273. https://doi.org/10.3390/polym6082247

9. Y.F. Zhu, Y.Q. Fu, T. Natsuki, Q.Q. Ni, Fabrication and microwave absorption properties of $BaTiO_3$ nanotube/polyaniline hybrid nanomaterials, Polymer

Composites 34 (2013) 265-273. https://doi.org/10.1002/pc.22409

10. S. Agnelli, V. Cipolletti, S. Musto, M. Coomb, L. Conzatti, S. Pandini, T. Riccò, M. Galimberti, Interactive effects between carbon allotrope fillers on the mechanical reinforcement of polyisoprene based nanocomposites, eXPRESS Polymer Letters 8 (2014) 436-449. DOI: 10.3144/expresspolymlett.2014.47

11. J.M. Thomassin, C. Jerome, T. Pardoen, C. Bailly, I. Huynen, C. Detrembleur, Polymer/carbon based composites as electromagnetic interference (EMI) shielding materials, Mater. Sci. Eng. R. 74 (2013) 211-232. https://doi.org/10.1016/j.mser.2013.06.001

12. Y. Chen, X. Liu, X. Mao, Q. Zhuang, Z. Xie, Z. Han, γ-Fe_2O_3–MWNT/poly(*p*-phenylenebenzobisoxazole) composites with excellent microwave absorption performance and thermal stability, Nanoscale 6 (2014) 6440-6447. DOI:10.1039/c4nr00353e

13. J. Xiang, J. Li, X. Zhang, Q. Ye, J Xu, Magnetic carbon nanofibers containing uniformly dispersed Fe/Co/Ni nanoparticles as stable and high-performance electromagnetic wave absorbers, Mater J Chem A 2 (2014) 16905-16914. https://doi.org/10.1039/c4ta03732d

14. D.H. Park, Y.K. Lee, S.S. Park, C.S. Lee, S.H. Kim, W.N. Kim, Effects of hybrid fillers on the electrical conductivity and EMI shielding efficiency of polypropylene/conductive filler composites, Macromolecular Research 21 (2013) 905-910. DOI: 10.1007/s13233-013-1104-8

15. T.W. Yoo, Y.K. Lee, S.J. Lim, H.G. Yoon, W.N. Kim, Effects of hybrid fillers on the electromagnetic interference shielding effectiveness of polyamide 6/conductive filler composites, J Mater Sci. 49 (2014) 1701-1708. DOI: 10.1007/s10853-013-7855-y

16. M. Chhowalla, H.S. Shin, G. Eda, L. Li, K.P. Loh, H. Zhang, The chemistry of two-dimensional layered transition metal dichalcogenide nanosheets, Nat. Chem. 5 (2013) 263-275. DOI:10.1038/nchem.1589

17. A.C. Patsidis, K. Kalaitzidou, D.L. Anastassopoulos, A.A. Vradis, G.C. Psarras, Graphite nanoplatelets and/or barium titanate/polymer nanocomposites: fabrication, thermomechanical properties, dielectric response and energy storage, Journal of the Chinese Advanced Materials Society 2 (2014) 207-221.

https://doi.org/10.1080/22243682.2014.937742

18. J. Wei, S. Zhang, X. Liu, J. Qian, J. Hua, X. Li, Q. Zhuang, In situ synthesis of ternary $BaTiO_3$/MWNT/PBO electromagnetic microwave absorption composites with excellent mechanical properties and thermostabilities, J. Mater. Chem. A. 3 (2015) 8205-8214. DOI: 10.1039/C5TA01410G

19. B. Wen, M.S. Cao, Z.L. Hou, W.L. Song, L. Zhang, M.M. Lu, H.B. Jin, X.Y. Fang, W.Z. Wang, J. Yuan, Temperature dependent microwave attenuation behavior for carbon-nanotube/silica composites, Carbon 65 (2013) 124-139. https://doi.org/10.1016/j.carbon.2013.07.110

20. L. Yu, Y. Zhu, C. Qian, Q. Fu, Y. Zhao, Y. Fu, Nanostructured Barium Titanate/Carbon Nanotubes Incorporated Polyaniline as Synergistic Electromagnetic Wave Absorbers, Journal of Nanomaterials (2016) Article ID 6032307, 8 pages http://dx.doi.org/10.1155/2016/6032307

21. D. Micheli, A. Vricella, R. Pastore, M. Marchetti, Synthesis and electromagnetic characterization of frequency selective radar absorbing materials using carbon nanopowders, Carbon 77 (2014) 756-774. https://doi.org/10.1016/j.carbon.2014.05.080

22. Z. Wang, K.J. Nelson, M.J. Jianjun, R. Linhardt, L. Schadler, Effect of High Aspect Ratio Filler on Dielectric Properties of Polymer Composites: A Study on Barium Titanate Fibers and Graphene Platelets, IEEE Transactions on Dielectrics and Electrical Insulation 19 (2012) 960-967. DOI: 10.1109/TDEI.2012.6215100

23. Y. Jin, N. Xia, R. Gerhardt, Enhanced Dielectric Properties of Polymer Matrix Composites with $BaTiO_3$ and MWCNT Hybrid Fillers using Simple Phase Separation, Nano Energy 10 (2016) 407-416. https://doi.org/10.1016/j.nanoen.2016.10.033

24. Y. Qing, X. Wang, Y. Zhou, Z. Huang, F. Luo, W. Zhou, Enhanced microwave absorption of multi-walled carbon nanotubes/epoxy composites incorporated with ceramic particles, Compos. Sci. Technol. 102 (2014) 161-168. https://doi.org/10.1016/j.compscitech.2014.08.006

25. L. Vovchenko, L. Matzui, V. Oliynyk, V. Launetz, Yu. Prylutskyy, D. Hui, Yu. Strzhemechny, Modified Exfoliated Graphite as a Material for Shielding Against Electromagnetic Radiation, Int. Journal of Nanoscience 7 (2008) 263-268. DOI: 10.1142/S0258191X08005419

26. O. Yakovenko, L. Matzui, Y. Perets, I. Ovsiienko, O. Brusylovets, L. Vovchenko, P. Szroeder, Effects of dispersion and ultraviolet/ozonolysis functionalization of graphite nanoplatelets on the electrical properties of epoxy nanocomposites, Nanophysics, Nanophotonics, Surface Studies, and Applications 39 (2016) 477-491 https://doi.org/10.1007/978-3-319-30737-4_39

27. J. Baker-Jarvis, E. Vanzura, W. Kissick, Improved Technique for Determining Complex Permittivity with the Transmission/Reflection Method, IEEE Transactions on Microwave Theory and Techniques 38 (1990) 1096-1103. DOI: 10.1109/22.57336

28. L. Vovchenko, L. Matzui, V. Oliynyk, V. Launetz, The Effect of Filler Morphology and Distribution on Electrical and Shielding Properties of Graphite-Epoxy Composites, Mol. Cryst. Liq. Cryst. 535 (2011) 179-188. https://doi.org/10.1080/15421406.2011.538335

29. Y.C. Li, S.C. Tjong, R.K. Li, Dielectric properties of binary polyvinylidene fluoride/barium titanate nanocomposites and their nanographite doped hybrids, eXPRESS Polymer Letters 5 (2011) 526-534. https://doi.org/10.3144/expresspolymlett.2011.51

30. D. Micheli, A. Delfini, R Pastore, M Marchetti, R Diana and G Gradoni, Absorption cross section of building materials at mm wavelength in a reverberation chamber, Meas. Sci. Technol. 28 (2017) 024001. https://doi.org/10.1088/1361-6501/aa53a1

31. R. Pastore, A. Delfini, D. Micheli, A. Vricella, M. Marchetti, F. Santoni, F. Piergentili, Carbon foam electromagnetic mm-wave absorption in reverberation chamber, Carbon 144 (2019) 63-71. https://doi.org/10.1016/j.carbon.2018.12.026

32. J. Joo, C.Y. Lee, High frequency electromagnetic interference shielding response of mixtures and multilayer films based on conducting polymers, J. Appl. Phys. 8, (2000) 513-518. https://doi.org/10.1063/1.373688

33. C. Min, D. Yu, J. Cao, G. Wang, L. Feng, A graphite nanoplatelet/epoxy composite with high dielectric constant and high thermal conductivity, Carbon 55 (2013) 116-125. https://doi.org/10.1016/j.carbon.2012.12.017

34. Z. Wang, J. Luo, G.L. Zhao, Dielectric and microwave attenuation properties of graphene nanoplatelet–epoxy composites, AIP Advances 4 (2014) 017139-9. https://doi.org/10.1063/1.4863687

35. L. Vovchenko, L. Matzui, V. Oliynyk, V. Launetz, Attenuation of electromagnetic radiation by graphite-epoxy composites, Phys Status Solidi. C 7 (2010) 1260-1263. https://doi.org/10.1002/pssc.200982961

36. L. Vovchenko, L. Matzui, V. Oliynyk, V. Launetz, O. Zhuravkov, Electrical and shielding properties of epoxy composites containing hybrid carbon fillers, Mat.-wiss. u. Werkstofftech. 44 (2013) 249-253. https://doi.org/10.1002/mawe.201300116

37. T. Prodromakis, C. Papavassiliou, Engineering the Maxwell–Wagner polarization effect, Appl. Surf. Sci. 255 (2009) 6989-6994. https://doi.org/10.1016/j.apsusc.2009.03.030

38. Nadir Abbas, Hee Taik Kim, Multi-Walled Carbon Nanotube/Polyethersulfone Nanocomposites for Enhanced Electrical Conductivity, Dielectric Properties and Efficient Electromagnetic Interference Shielding at Low Thickness, Macromolecular Research 24 (2016) 1084-1090. DOI: 10.1007/s13233-016-4152-z

39. R. Dosoudil, M. Usáková, J. Franek, J. Sláma, A. Grusková, Particle Size and Concentration Effect on Permeability and EM-Wave Absorption Properties of Hybrid Ferrite Polymer Composites, IEEE Trans. Magn. 46 (2010) 436-439.
DOI: 10.1109/TMAG.2009.2033347

40. R. Hu, G. Tan, X. Gu, S. Chen, C. Wu, Q. Man, C. Chang, X. Wang, RW. Li, S. Che, L. Jiang, Electromagnetic and microwave-absorbing properties of Co-based amorphous wire and Ce2Fe17N3-δ composite, J Alloys Compd 730 (2018) 255-260. https://doi.org/10.1016/j.jallcom.2017.09.302

41 X. Bai, Y. Zhai, Y. Zhang, Green Approach To Prepare Graphene-Based Composites with High Microwave Absorption Capacity, J Phys Chem C. 115 (2011) 11673-11677. https://doi.org/10.1021/jp202475m

42. Y. Akinay, F. Hayat, Y. Kanbur, H. Gokkaya, S. Polat, Comparison of Microwave Absorption Properties Between BaTiO3/Epoxy and $NiFe_2O_4$/Epoxy Composites, Polym Composite 39 (2017) E2143-E2148.
https://doi.org/10.1002/pc.24497

43. L. Yu, Y. Zhu, Y. Fu, Flexible composite film of aligned polyaniline grown on the surface of magnetic barium titanate/polyvinylidene fluoride for exceptional microwave absorption performance, RSC Adv. 7 (2017) 36473-36481.
https://pubs.rsc.org/en/content/articlelanding/2017/ra/c7ra05744j#!divAbstract

44. Q.-Q. Ni, Y.-F. Zhu, L.-J. Yu, Y.-Q. Fu, One-dimensional carbon nanotube@barium titanate@polyaniline multiheterostructures for microwave absorbing application, Nanoscale Res Lett 10 (2015) 174-8
https://nanoscalereslett.springeropen.com/articles/10.1186/s11671-015-0875-6

45. G.P. Kar, S. Biswas, R. Rohini, S. Bose, Tailoring the dispersion of multiwall carbon nanotubes in co-continuous PVDF/ABS blends to design materials with enhanced electromagnetic interference shielding, J Mater Chem A 3 (15) (2015) 7974-7985.
https://pubs.rsc.org/en/content/articlelanding/2015/ta/c5ta01183c#!divAbstract

46. C.R. Paul, Electromagnetics for Engineers (Wiley, Hoboken, NJ., 2004).

47. Z. Wang, G.L. Zhao, Microwave absorption properties of carbon nanotubes-epoxy composites in a frequency range 2-20GHz, Open J. Compos. Mater. 3 (2013) 17. DOI: 10.4236/ojcm.2013.32003

48. A.A. Eddib, D.D.L. Chung, The importance of the electrical contact between specimen and testing fixture in evaluating the electromagnetic interference shielding effectiveness of carbon materials, Carbon 117 (2017) 427-436.
https://doi.org/10.1016/j.carbon.2017.02.091

49. Z. Liu, G. Bai, Y. Huang, Y. Ma, F. Du, F. Li, T. Guo, Y. Chen, Reflection and absorption contributions to the electromagnetic interference shielding of single-walled carbon nanotube/polyurethane composites, Carbon 45 (2007) 821-827. https://doi.org/10.1016/j.carbon.2006.11.020

50. S. Kashi, S. Ali Hadigheh, R. Varley, Microwave Attenuation of Graphene Modified Thermoplastic Poly(Butylene adipate-*co*terephthalate) Nanocomposites, Polymers 10 (2018) 582-14; doi:10.3390/polym10060582

51. F. Shahzad, S. Yu, P. Kumar, J.-W. Lee, Y.-H. Kim, S. M. Hong, and C. M. Koo, Sulfur-doped graphene laminates for EMI shielding applications, J Mat Chem C 38 (2015) 9802-9810.
https://pubs.rsc.org/en/content/articlelanding/2015/tc/c5tc02166a#!divAbstract

52. M. H. Al-Saleh, Electrical, EMI shielding and tensile properties of PP/PE blends filled with GNP:CNT hybrid nanofiller. Synth Met 217 (2016) 322–330. https://doi.org/10.1016/j.synthmet.2016.04.023

53. M. Verma, S.S. Chauhan, S.K. Dhawan, V. Choudhary, Graphene nanoplatelets/carbon nanotubes/polyurethane composites as efficient shield against electromagnetic polluting radiations, Compos Part B: Eng. 120 (2017) 118-27. https://doi.org/10.1016/j.compositesb.2017.03.068

54. M. Jahan, R. Osuemeshi Inakpenu, K. Li, G. Zhao, Enhancing the Mechanical Strength for a Microwave Absorption Composite Based on Graphene Nanoplatelet/Epoxy with Carbon Fibers, Open J Compos Mater. 9 (2019) 230-248. http://www.scirp.org/journal/ojcm

55. S. Singh Chauhan, P. Verma, R. Singh Malik, V. Choudhary, Thermomechanically stable dielectric composites based on poly(ether ketone) and $BaTiO_3$ with improved electromagnetic shielding properties in X-band, J Appl Polym Sci. 135 (2018) 46413-11p. https://doi.org/10.1002/app.46413

56. N. Joseph, S.K. Singh, R.K. Sirugudu, V.R.K. Murthy, S. Ananthakumar, M.T. Sebastian, Effect of silver incorporation into PVDF barium titanate composites for EMI shielding applications, Mater Res Bull. 48 (2013) 1681-1687. http://dx.doi.org/10.1016/j.materresbull.2012.11.115

57. P.Z. Liu, L. Zhang, W. F. Wang, W. Cheng, D. F. Li and D.Y. Zhang, Synthesis and Electromagnetic Shielding Properties of Graphene-Fe_3O_4-$BaTiO_3$/Silicone Rubber Nanocomposites, Mater Sci Forum 950 (2018) 97-102. https://doi.org/10.4028/www.scientific.net/MSF.950.97

Highlights

- Ternary epoxy composites filled with a mixture of GNPs and $BaTiO_3$ particles
- Electrical conductivity of 0.013 S/m at 6 wt.% of GNP
- Better dispersion of GNP in GNP/BT/epoxy composite results in increased permittivity
- Increase of EMR shielding due to enhanced electric loss for higher GNP content
- Reflection loss in GNP/BT/epoxy versus GNP content and sample thickness